



Shift of subtropical transport barriers explains observed hemispheric asymmetry of decadal trends of age of air

Gabriele P. Stiller¹, Federico Fierli², Felix Ploeger³, Chiara Cagnazzo², Bernd Funke⁴, Florian J. Haenel¹, Thomas Reddmann¹, Martin Riese³, and Thomas von Clarmann¹

¹Karlsruhe Institute of Technology, IMK, P.O.B. 3640, 76021 Karlsruhe, Germany

²National Research Council, Institute for Atmospheric Sciences and Climate, Via Fosso del Cavaliere 100, 00199 Rome, Italy

³Institute for Energy and Climate Research - Stratosphere (IEK-7), Forschungszentrum Jülich, 52425 Jülich, Germany

⁴Instituto de Astrofísica de Andalucía (CSIC), Glorieta de la Astronomía s/n, 18008 Granada, Spain

Correspondence to: Gabriele P. Stiller (gabriele.stiller@kit.edu)

Abstract. In response to global warming the Brewer-Dobson circulation in the stratosphere is expected to accelerate and the mean transport time of air along this circulation to decrease. This would imply a negative stratospheric age of air trend, i.e. an air parcel would need less time to travel from the tropopause to any point in the stratosphere. Age of air as inferred from tracer observations, however, shows zero to positive trends in the Northern midlatitude stratosphere and zonally asymmetric patterns.

5 Using satellite observations and model calculations we show that the observed latitudinal and vertical patterns of the decadal changes of age of air in the lower to middle stratosphere during 2002–2012 are predominantly caused by a southward shift of the circulation pattern of about 5 degrees. After correction for this shift, the observations reveal a hemispherically almost symmetric decrease of age of air in the lower to middle stratosphere up to 800 K of up to -0.25 years over the 2002-2012 period with strongest decrease in the Northern tropics. This net change is consistent with long-term trends from model predictions.

10 1 Introduction

An acceleration of the Brewer-Dobson circulation as a consequence of global warming has been predicted by climate models (Austin et al., 2007; Austin and Li, 2006; Garcia and Randel, 2008; McLandress and Shepherd, 2009; Oman et al., 2009; SPARC CCMVal, 2010). The mean age of stratospheric air (AoA), used as a diagnostic of the strength of the Brewer-Dobson circulation (Vaugh and Hall, 2002), is expected to decrease since an air parcel would need less time from the stratospheric entry point at the tropical tropopause to its actual location (Vaugh, 2009). Balloon-borne inert tracer measurements (CO₂ and SF₆), however, yielded zero to positive age of air trends in the Northern midlatitudinal stratosphere for 1975-2005 (Engel et al., 2009), which seemed to be in conflict with the expectation. A global analysis of age of air trends derived from MIPAS satellite data for 2002 to 2012 supported these results for Northern midlatitudes but provided, beyond this, a global picture which resisted any easy explanation (Stiller et al., 2012; Haenel et al., 2015). Negative trends of mean age of air were found for large parts of the Southern middle stratosphere and the tropics, revealing a dipole-like structure of mean age of air trends with opposite signs in the two hemispheres. Similar hemispheric asymmetries of trends of stratospheric trace species were derived from other observational data sets by various groups, corroborating the results from the MIPAS AoA analysis, e.g. for



ozone (Eckert et al., 2014; Gebhardt et al., 2014; Nedoluha et al., 2015a, b; Pawson et al., 2014), hydrogen fluoride (Harrison et al., 2016), hydrogen chloride (Mahieu et al., 2014), (H)CFCs (Chirkov et al., 2016; Kellmann et al., 2012), nitrous oxide (Nedoluha et al., 2015a), and carbonyl sulfide (Glatthor et al., 2016).

The AoA trends in the lowermost stratosphere below 380 K were found to be negative equatorwards of 40° in both hemispheres, but slightly positive polewards of 40° and between 380 and 420 K for the lower latitudes (Ploeger et al., 2015b). This difference between trends in low and high latitudes hints at a decoupling of the deep and the shallow branch of the Brewer-Dobson circulation, consistent with the general picture presented in Birner and Bönisch (2011); Bönisch et al. (2011). Alternative explanations point at the importance of mixing processes (Ray et al., 2010; Garny et al., 2014; Ploeger et al., 2015b). Neither of these hypotheses, however, can explain the partly opposed trends in both hemispheres as inferred from satellite measurements of SF₆ (Stiller et al., 2012; Haenel et al., 2015).

This paper is organised as follows: After a description of data and methods used (Section 2), we determine the positions of the subtropical transport barriers and their change over time (Section 3). We apply the derived shifts to tracer distributions (Section 4) and age of air distributions (Section 5) and demonstrate that the observed temporal changes can be emulated by the southward shift of the circulation pattern. In Section 6 we discuss our findings and their implications in the context of other work. In the conclusions (Section 7) we summarise our main findings and discuss their implications for other approaches to determine a change in the Brewer-Dobson circulation.

2 Data and methods

We have used satellite data from MIPAS and MLS, CLaMS model simulations and ERA-Interim reanalysis data in our work.

2.1 MIPAS data

The Michelson Interferometer for Passive Atmospheric Sounding (MIPAS) on the Environmental Satellite (Envisat) (Fischer et al., 2008) has been used to measure global stratospheric SF₆ distributions. Monthly zonal mean SF₆ distributions were converted into age of air distributions from which decadal age trends have been inferred (Stiller et al., 2012). A revised set of age of air trends based on improved SF₆ retrievals (Haenel et al., 2015) and covering the full measurement period of 2002 to 2012 is used here. N₂O global distributions from MIPAS for 2002 to 2012 have been used to derive the positions of the subtropical transport barriers. The original data represented on a geometric altitude grid have been interpolated to eight potential temperature levels between 520 and 1100 K. The retrieval of N₂O from MIPAS observations is described by Plieninger et al. (2015), while validation of the N₂O data set is presented by Plieninger et al. (2016).

2.2 MLS data

N₂O global distributions for 2004 to 2014 from Aura/MLS have been used to derive the position of the subtropical transport barriers. MLS data version 3.30 has been retrieved from the Jet Propulsion Laboratory data server and interpolated to eight



potential temperature levels between 520 and 1100 K. The retrieval and validation of MLS N₂O data is described in Lambert et al. (2007).

2.3 Model calculations

The model simulations presented in this paper have been carried out with the Chemical Lagrangian Model of the Stratosphere CLaMS (McKenna et al., 2002). The advective part of transport in CLaMS is based on three-dimensional forward trajectories, driven by ERA-Interim reanalysis winds. As CLaMS uses potential temperature as vertical coordinate above $\sigma = 0.3$ (where $\sigma = p/p_s$ is the orography following vertical coordinate near the surface, with p pressure and p_s surface pressure), the vertical transport in the model is driven by the total diabatic heating rate, taken from the reanalysis forecast. In addition, a parameterisation of small-scale atmospheric mixing is included in CLaMS, depending on the deformation rate of the large-scale flow.

The model age of air used here has been calculated from a ‘clock-tracer’, an inert tracer with a linearly increasing source in the orography-following lowest model layer (boundary layer). Further details about the model set-up used here are given by Pommrich et al. (2014).

2.4 Trace gas gradient genesis

Miyazaki and Iwasaki (2007) presented a method to separate the tendency of latitudinal trace gas gradients along an isentrope into the effects of mean residual circulation and eddy transport. Mean transport may cause a sharpening of gradients related to horizontal ‘stretching’ and vertical ‘shearing’, or a shift of gradients by meridional and vertical advection. Eddy transport may sharpen gradients at the edges of strong mixing regions (e.g., the surf zone) due to the ‘stair-step’ effect or may dilute gradients due to the ‘smoothing’ effect. We performed this separation for CLaMS simulated N₂O fields and analysed all relevant terms. Presented in the paper is the net trace gas gradient tendency, the net ‘genesis’ term (Fig. 3).

3 The temporal evolution of the positions of the subtropical transport barriers

For deriving the positions of the subtropical transport barriers, we follow the method described by Sparling (2000). Using this approach, Palazzi et al. (2011) analyzed the probability density functions (PDFs) of long-lived tracer observations from four different satellite instruments over the years 1992 to 2009. The minimum of the tracer PDFs identifies a region where transport is inhibited and is hence used to diagnose the latitudinal positions of the barriers. As opposed to latitudinal gradients, the position of the PDF minima do not depend on the particular tracer used and are immune against biases between different data bases. Palazzi et al. (2011) found a strong dependence of the transport barrier positions on the seasonal cycle and a significant impact of the phase of the quasi-biennial oscillation (QBO). We apply their method to a decadal analysis of the subtropical transport barrier positions by including longer periods of observational data and model simulations: we use N₂O distributions from MIPAS (2002 to 2012), MLS (2004 to 2014), and from the Lagrangian transport model CLaMS driven by ERA-Interim reanalyses (1992 to 2014) (Fig. 1).

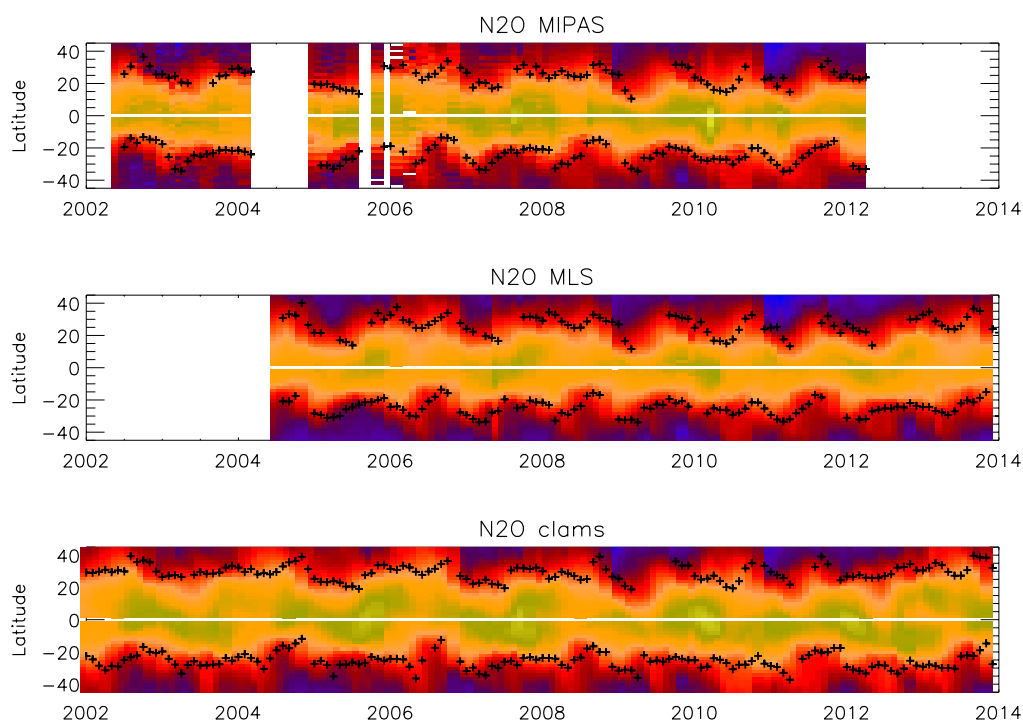


Figure 1. Time series of zonal N_2O distributions at the 600 K potential temperature level from MIPAS observations (top panel), MLS observations (middle panel), and CLaMS model simulations driven by ERA-Interim reanalyses (bottom panel). The black crosses indicate the positions of the subtropical transport barriers derived with the method by Palazzi et al. (2011).

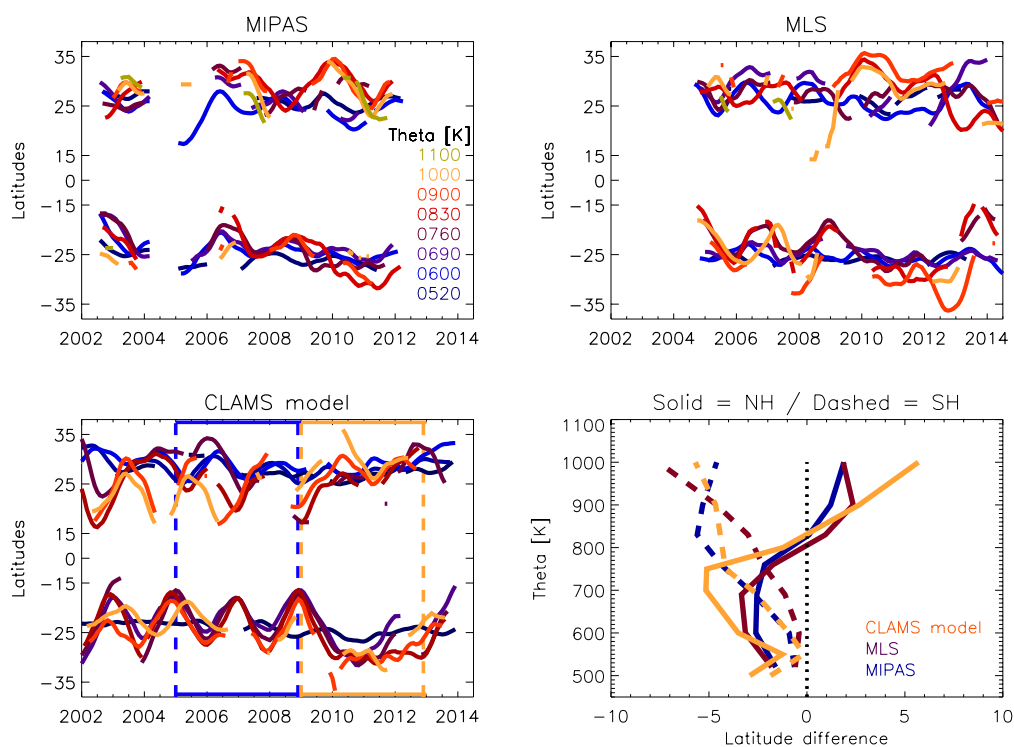


Figure 2. Positions of the subtropical transport barriers over time for eight potential temperature levels between 520 and 1100 K (colour coding see legend) from N_2O monthly zonal mean distributions observed by MIPAS (top left), MLS (top right), and simulated by CLaMS (bottom left). The bottom right panel provides the vertical profiles of the shifts of the transport barrier positions determined as the difference of the mean positions of the 2005 – 2008 versus 2009 – 2012 period (vertical dashed lines in the bottom left panel).



We determined the shift of the latitudinal positions of the transport barriers for eight levels of potential temperatures between 500 and 1000 K (appr. 19–36 km) by comparing the mean latitudinal positions of two time intervals: 2005–2008 (period I in the following) versus 2009–2012 (period II) (Fig. 2). The two periods were selected because data coverage was best for them, and a change in the barrier positions is obvious between the two periods. For both observational data sets and the CLaMS simulations a consistent picture is obtained: below 800 K, the Northern subtropical transport barrier moved towards the South by about -3° from period I to period II, while above 800 K, the emerging shifts are northward. The Southern subtropical transport barrier, however, moved southward for all potential temperature levels, with shift values increasingly negative with increasing altitude. This results in a southward shift and small narrowing of the tropical pipe below 800 K and a significant widening of the tropical pipe above.

In order to demonstrate the consistency of the transport barrier positions determined by us with well-known dynamical mechanisms discussed earlier in literature (Shuckburgh et al., 2001; Palazzi et al., 2011; Miyazaki and Iwasaki, 2007), we compare the transport barrier positions derived above with the positions of the maximum tracer gradient regions according to Miyazaki and Iwasaki (2007) and with the autumn/spring positions of the turnaround latitudes ($\bar{w}^* = 0$) derived from ERA-Interim reanalysis data (see Fig. 3). In general, all diagnostics for the transport barrier positions exhibit a large intraseasonal and interannual variability, with the zonal-mean zonal winds (QBO) (Shuckburgh et al., 2001) and the latitudinal gradients in the residual circulation and diffusion (Miyazaki and Iwasaki, 2007) playing major roles as drivers. The turnaround latitudes ($\bar{w}^* = 0$) may also provide information on the position of the subtropical transport barriers as these separate the upwelling motion in the tropical pipe from the downward transport in the surf zones; however, the latitudinal positions of turnaround latitudes are not expected to be always identical with those of the transport barriers. For the Northern hemisphere, the positions of the turnaround latitudes (red dashed lines in Fig. 3) for autumn and spring are in good agreement with the positions of the subtropical transport barriers derived from satellite tracer observations, while for the Southern hemisphere, neither the positions nor the shift agree well. At the intra-seasonal timescales, the turnaround latitude positions are related to the variations of the maximum tracer gradient regions (black contours in Fig. 3) that are identified as gradient generator by Miyazaki and Iwasaki (2007); maximum gradients are in turn correlated with minimum PDFs. Indeed, the positions of the gradient genesis regions and their shifts agree well with those derived from satellite tracer observations.

All three quantities indicating the positions of the subtropical transport barriers show a rather sudden shift towards the South around the year 2009 (\bar{w}^* only for the Northern hemisphere). This shift is most clearly reflected in the locations of the genesis areas for the meridional N_2O -gradients. The analyses of the location of the gradient genesis and the \bar{w}^* turnaround latitudes demonstrate that changes in the circulation are responsible for the shifts found in the tracer abundance fields observed by MLS and MIPAS, and that this process is also contained in ERA-Interim reanalysis data.

4 Shift of the global circulation pattern

The meridional gradient determining the subtropical transport barrier is generated by latitudinal variations in \bar{w}^* , by the strength of the mixing and wind shear (Miyazaki and Iwasaki, 2007). Hence a shift in the position of the PDF minima (i.e. minimum

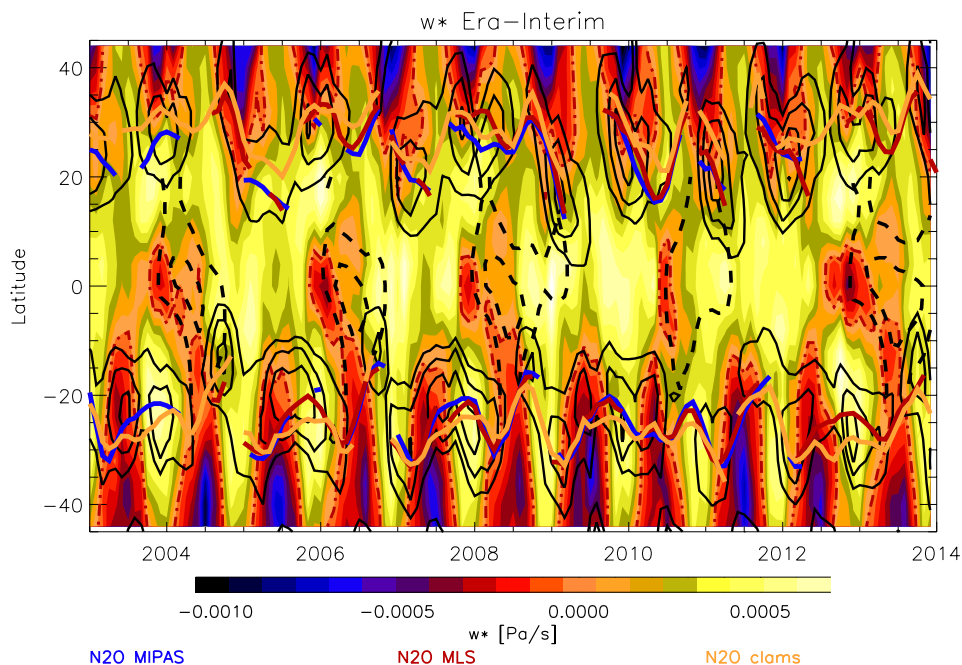


Figure 3. Positions of the subtropical transport barriers over time at 600K compared to other dynamical quantities providing a measure for the position of the tropical pipe: the blue, red, and orange solid lines are the positions of the subtropical transport barriers from MIPAS, MLS and CLaMS data, respectively, derived with the method of Palazzi et al. (2011); the color coding indicates the values of \bar{w}^* (see color bar); the turnaround latitude (e.g. $\bar{w}^* = 0$) is indicated as red dashed line; the latitude regions of meridional gradient genesis are indicated as black contour lines. Black dashed lines mark zero zonal-mean zonal wind (QBO phases).

transport) may be related to a shift in the entire circulation pattern. If the shift of the tropical pipe was indicative for a shift of the complete circulation pattern in this altitude regime, we would expect, at first order, the zonal distribution pattern of any long-lived tracer to be shifted by the same amount. This is because the zonal mean distribution of a long-lived tracer in the stratosphere is predominantly determined by the residual circulation and the additional eddy mixing. We therefore used the CLaMS N_2O zonal mean distribution for the first period of interest (period I, 2005–2008), and applied altitude-dependent latitudinal shifts according to the values derived for the transport barrier positions. This was done for all latitudes polewards of 10°N/S . At tropical latitudes appropriate shift values have been calculated by linearly interpolating from the derived values at 10°N/S , and the distributions have been accordingly shifted. The shift effect to the distributions has finally been calculated by subtracting the unshifted original distribution from the shifted distribution. The altitude/latitude pattern of these differences is then compared to the altitude/latitude pattern of N_2O decadal changes as modelled with CLaMS (Fig. 4). Equatorwards of about 60°N/S , the pattern of the CLaMS-modelled decadal changes of the zonal mean distribution of N_2O is explained to a large degree by the shift of the N_2O zonal mean distribution. Overall, the remarkable agreement of the patterns indicates that a shift of the entire circulation pattern is largely responsible for the changes in the tracer distribution. Remaining differences in the change versus shift patterns hint towards other competing processes taking place as well in reality. The absolute amounts of the changes are larger than those derived by shifting the distribution, hinting also towards such competing processes.

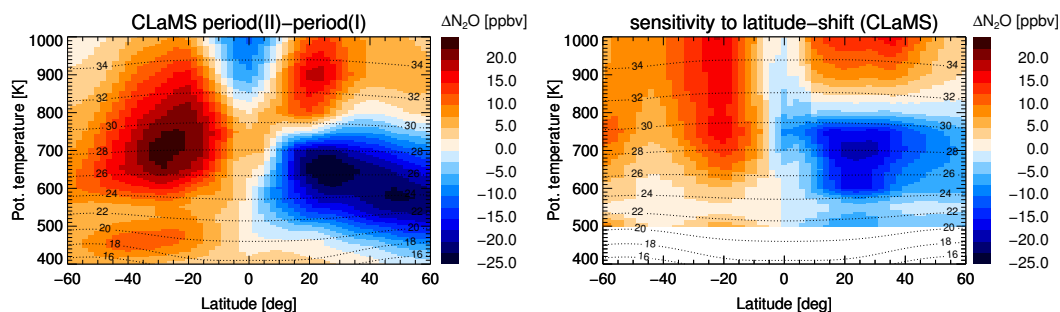


Figure 4. Difference of CLaMS zonal mean N_2O distributions between the periods I and II (left), compared to the effect of a shift of the N_2O zonal mean distribution of period I according to the altitude dependent latitude shifts of the subtropical transport barriers as derived for CLaMS (Fig. 2, bottom right panel, orange lines) (right).

Similar hemispheric dipole patterns in linear trends of stratospheric tracers, or in differences of tracer distributions between two periods, have been observed for a number of trace species from several observations: Mahieu et al. (2014) found increasing HCl volume mixing ratios in the Northern and decreasing volume mixing ratios in the Southern hemisphere between 2005/6 and 2010/11 for 10–25 km altitude and related this to a respective change of age of air derived from SLIMCAT and KASIMA model simulations. Harrison et al. (2016) detected a similar dipole pattern in the change of HF between 2004 and 2012. Kellmann et al. (2012) found CFC-11 and CFC-12 changes over the period of 2002 to 2012 that were smaller than the trends at the surface for the Northern hemisphere and larger than the surface trends in the Southern hemisphere. Similar deviations from surface trends were found for HCFC-22 for the period 2005–2012 (Chirkov et al., 2016). Nedoluha et al. (2015a) and Nedoluha et al. (2015b) found hemispheric asymmetries and dipole patterns in trends of N_2O and ozone for the period 2004–2013 by analyzing Aura/MLS data. Dipole patterns in ozone trends were also seen in ozone data from other satellite instruments (MIPAS, SCIAMACHY) for 2002–2012 (Eckert et al., 2014; Gebhardt et al., 2014). The signs of all these observed changes are consistent with a southward shift of the tracer distributions. It is therefore very likely that all these observations can be explained by the southward shift of the circulation pattern as well.

5 Effect of the shift of the stratospheric circulation pattern on observed and modelled age of air

The shift of the circulation pattern to the South below 800 K and the widening of the tropical pipe above should be detectable also in the age of air distribution in the stratosphere. We apply the latitudinal shift as detected from the observed and modelled subtropical transport barrier positions to the global zonally averaged age of air distribution of period I derived from MIPAS observations and modelled by CLaMS.

For MIPAS, the dipole-like structure in the age of air decadal change in the middle stratosphere between 500 and 800 K is well reproduced by the effect of the shift of the transport barrier positions, applied to the distribution of period I (Fig. 5, top right panel). However, there remain differences in the upper stratosphere above 800 K and in the Southern hemisphere



southward of 40° S. Both regions are strongly affected by advection of SF₆-depleted mesospheric air. Since the amount of SF₆ depletion in the mesosphere is proportional to the available SF₆ abundance, the increase of SF₆ in the atmosphere itself leads to an increasing SF₆ loss which in turn appears as a non-real additional positive age of air trend (Stiller et al., 2012; Haenel et al., 2015). This artefact may outweigh the negative change of age of air. Another explanation for this observed discrepancy could be that the widening of the tropical belt above 800 K does not affect the mid-latitudes in a similar way than the shift of the subtropical transport barriers at lower altitudes. Further, the observed change is negative in the Northern tropics and the dipole is asymmetric to the equator, while the age of air changes produced by the shift of the distributions are symmetric to the equator, as expected from the symmetric age of air distribution itself.

For CLaMS age of air trends, the situation is clearer, and the model simulations confirm the findings from the observations. Below 800 K, the pattern of the age of air change between period I and period II (Fig. 5, bottom left panel) has a similar dipole structure as the MIPAS observations, with widely negative trends in the Southern hemisphere, and positive trends in the Northern middle stratosphere (Ploeger et al., 2015b). In contrast to the MIPAS data, we find negative trends in the Northern upper stratosphere; this is because CLaMS uses a perfect clock tracer for age of air, that is not affected by chemical loss as SF₆. The shift of the circulation pattern to the South reproduces the pattern of the trends extremely well (Fig. 5, bottom right panel). However, similar to N₂O (Fig. 4), the changes due to the shift are weaker than the modelled changes, hinting towards additional competing processes. The negative change in the Northern hemisphere above 800 K is explained by the widening of the tropical pipe there (see Fig. 2, bottom right panel). In contrast to the MIPAS observations, the CLaMS changes are positive in the Northern tropics below 800 K.

The good general agreement between MIPAS and CLaMS confirms that the derived shift of the tropical pipe and the surf zones is represented as well in the ERA-Interim meteorological data that are used to drive CLaMS. However, observed differences like the negative change in the Northern tropics hint to competing processes which cannot be explained by the shift of the circulation pattern alone.

6 Discussion

We have shown that the observed dipole pattern in changes of stratospheric age of air during the last decade (2002–2012) (Stiller et al., 2012; Haenel et al., 2015), with negative changes in the Southern hemisphere and positive changes in the Northern hemisphere can be explained to a large part by a shift of the stratospheric circulation pattern. Both MLS and MIPAS satellite observations and the ERA-Interim reanalysis show clear evidence for this shift. Indications for the shift are the changes of the positions of the subtropical transport barriers. The transport barriers have been shown to move southwards below 800 K in both hemispheres over the period 2005 to 2012 by about 5°. Above 800 K, the transport barriers diverge, leading to a substantial widening of the tropical pipe at these higher levels. The positions of the transport barriers have been derived from both observational and modelled tracer fields and provide a consistent picture, indicating that ERA-Interim meteorological data that drive the model calculations exhibits this shift of the circulation pattern as well. Moreover, comparison to direct diagnostics from ERA-Interim, the \bar{w}^* turnaround latitude and the latitude of the meridional trace gas gradient genesis (Miyazaki and

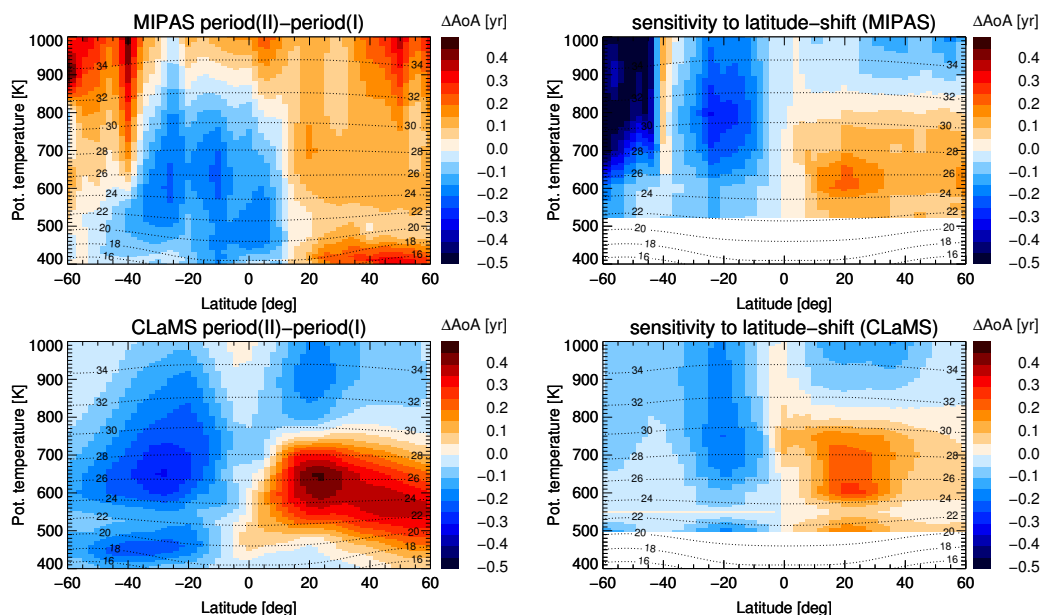


Figure 5. Top: Difference of MIPAS zonal mean age of air distributions between the periods I and II (left), compared to the effect of a shift of the zonal mean age of air distribution of period I according to the altitude dependent latitude shifts of the subtropical transport barriers as derived for MIPAS (Fig. 2, bottom right panel, blue lines) (right). Bottom: The same for CLaMS zonal mean age of air.

Iwasaki, 2007) demonstrate consistency of our findings regarding the shifts of the transport barrier positions with the general dynamical mechanisms.

We cannot exclude additional influences on the stratospheric trace gas distributions, like potential effects of changes in the upward mass flux due to a changing volume of the upwelling region related to the southward shift, or of changes in the permeability in the subtropical transport barriers. However, the good agreement between the decadal change and the effect of shifting the global trace gas distributions provides strong evidence that the pure shift effect is the dominant cause for the observed age of air and trace gas changes during the last decade.

The positions and latitudinal extensions of the surf zones that are separated from the tropical pipe by the subtropical transport barriers are determined by the latitude where planetary waves can propagate into the stratosphere and break there. The propagation of planetary waves is hindered by the tropical easterly jet and, therefore, the positions of the subtropical mixing barriers are closely related to the position of the jet. Hence, the observed southward shift might be related to changes in the position of the jet, similar to the findings regarding longer term trends in jet positions by Hardiman et al. (2013).

Decadal changes, as discussed here, may be largely influenced by natural variability. As a prominent mode of variability in the lower stratosphere, the Quasi-Biennial Oscillation (QBO) affects wave propagation and likely the position of the subtropical transport barriers, with planetary waves and associated mixing penetrating to lower latitudes during westerly phase (Gray and III, 1999; Shuckburgh et al., 2001; Palazzi et al., 2011). Similarly, Calvo et al. (2010) demonstrated that sea surface temperature

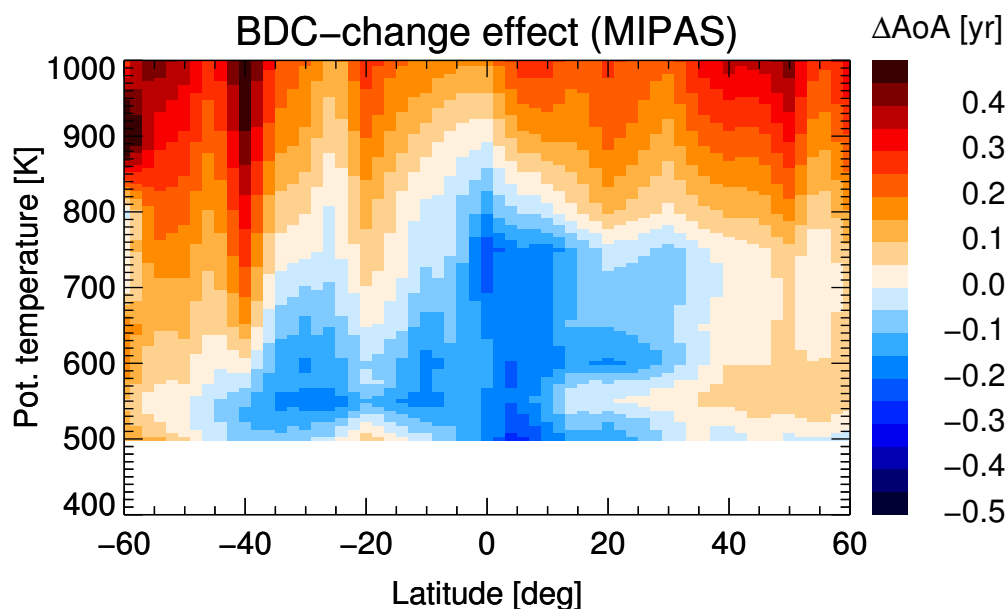


Figure 6. Difference between the observed age of air changes from MIPAS between period I and II and the effect of the derived shift of the circulation pattern. These remaining changes cannot be explained by the shift of the circulation pattern and are caused by competing processes.

anomalies related to strong El Niño and La Niña events also impact the propagation of planetary waves into the stratosphere and have the potential to shift the positions of the subtropical jets and the surf zones. A very recent model study of Garfinkel et al. (2016) shows that climate model simulations may include members with increasing mean age in the NH. Therefore a realistic representation of natural variability in model simulations is crucial if comparisons of decadal circulation trends with observations are made.

While the cause for the circulation shift is an important research issue in itself, our analysis provides evidence that the age of air observations by MIPAS do not generally contradict the theoretical expectation of an accelerated Brewer-Dobson circulation but that the latter effect can simply be masked by competing processes of possibly shorter time scales. Figure 6 shows the remaining age of air trend from MIPAS after subtracting the part which can be explained by the shift of the circulation pattern.

- After this correction the dipole pattern has disappeared and the change of age of air follows widely the idea of an accelerated deep branch of the Brewer-Dobson circulation below 800 K at tropical to mid-latitudes. The negative trend could indicate either an acceleration of the BDC (accompanied by related changes of isentropic mixing, see e.g. Ploeger et al. (2015a)) or an additional upward shift of the circulation pattern as suggested by Oberländer-Hayn et al. (2016). In any case, the strongest negative trend of about -0.25 years/decade occurs in the Northern tropics and is consistent with trends derived from model calculations (e.g., Waugh, 2009). The strong positive changes above 800 K, however should be taken with caution, because, as explained earlier, an artefact due to in-mixing of mesospheric SF₆-depleted air, leading to artificial positive age trends, cannot be excluded.



7 Conclusions

We have demonstrated that the observed spatial pattern of the trend of stratospheric age of air from 2002 to 2012 with different signs on the two hemispheres can be explained, to a large part, by a southward shift of the stratospheric circulation pattern between the potential temperature levels of approximately 500 and 800 K. This hypothesis of a southward shift is corroborated by a simultaneous southward movement of the subtropical transport barriers over this period in the order of zero to five degrees, dependent on altitude. We have demonstrated this southward shift of the subtropical transport barriers by means of various measures of their latitudinal positions: first, we have derived the latitudinal positions from tracer distributions from independent satellite observations; then, in order to demonstrate the consistency of these positions with the general dynamical mechanisms, we have compared the positions to the turnaround latitudes of the residual circulation vertical velocity \bar{w}^* ; and to the latitudinal positions of the regions of meridional trace gas gradient genesis following Miyazaki and Iwasaki (2007).

Further, we have shown that the chemistry-transport model CLaMS driven by ERA-Interim meteorology reproduces the observed southward shift of the transport barriers. This confirms that the ERA-I reanalysis data contain information on the dynamical processes leading to the observed shift. The modelled changes of zonal mean tracer distributions like N_2O can largely be emulated by shifting the distributions to the South, which shows that not only the mixing barriers but the entire stratospheric circulation pattern has experienced this southward shift. The fact that the full hemispheric circulation, or at least the positions of the surf zones over their full latitudinal extensions, are coupled to the positions of the subtropical transport barriers is a new and interesting finding in itself.

Both the observed and modelled mean age of air trend patterns can be emulated by applying the same southward shift to the age of air zonal mean distribution. The age of air change in the two hemispheres is therefore to be understood as a local change: the age of air in a certain latitude band changes according to the shift of latitudinal position of the circulation; it does not directly hint towards an acceleration or deceleration of the Brewer-Dobson circulation or related isentropic mixing effects. Indeed, Ploeger et al. (2015a) have shown that the age of air changes shown in Fig. 5 (bottom left) are mainly due to a trend in aging by mixing; again, this trend is caused by a shift of the latitudinal regimes where aging by mixing takes place. In contrast to this, the remaining observed AoA trend after correction for shift effects (Fig. 6) seems to indicate true changes in the residual circulation, either due to changes in the residual transport times or the isentropic mixing or both.

The identification of potential mechanisms responsible for the observed northward/southward movement of the subtropical transport barrier and surf zones is an interesting research topic on its own and beyond the scope of this paper. We have shown that such kind of processes acting on time scales of decades may have extensive impact on the distribution of tracers and the stratospheric age of air. They cannot be ignored when observational data are to be interpreted. This is particularly true if the analysis is fixed to certain latitude bands as it is often done to derive changes in the tropical uplift from tracer distributions like ozone. Ignoring a latitudinal shift of the upwelling region over time may lead to erroneous conclusions about the change of the strength of the Brewer-Dobson circulation. Vice versa, trends of age of air or tracers cannot fully be derived from observations within an oversimplified picture of a scalar and latitudinally fixed acceleration or slowing down of the Brewer-Dobson circulation. In particular, an adequate representation of natural variability in models appears as a necessary



prerequisite, and it is important to take the natural variability both in the models and observational data into account when making comparisons, especially for trends over relatively short periods.

8 Data availability

MIPAS data are available from <http://www.imk-asf.kit.edu/english/308.php> (upon registration) and from the corresponding author (Gabriele.Stiller@kit.edu). MLS data are available from <https://mirador.gsfc.nasa.gov> (upon registration). The CLaMS model data may be requested from the corresponding author (f.ploeger@fz-juelich.de). ERA-I data were retrieved directly from the ECMWF web site <http://www.ecmwf.int/en/research/climate-reanalysis/era-interim>.

Author contributions. G.P.S. initiated the study, coordinated the various analyses and wrote the manuscript. F.P. set up and analysed CLaMS model simulations, prepared most of the figures, and contributed to the analysis of the results and the writing of the manuscript. F.F. derived the positions of the transport barriers from satellite data, analysed ERA-Interim data, and contributed to the analysis of the results and the writing of the manuscript. C.C. contributed to the analysis and interpretation of the ERA-Interim-derived diagnostics. B.F. initiated the study by discussions on the structure of trace gas trends, and contributed to all further discussions and the writing of the manuscript. F.H. provided MIPAS satellite data of age of air. T.R. provided expert advice on age of air in model simulations. M.R. contributed to the analysis and interpretation of the results. T.v.C. provided expert advice with satellite data, and contributed to the analysis and interpretation of the results and to the paper writing.

Acknowledgements. Part of this work was funded by the German Federal Ministry of Education and Research under grant no. 01LG1221B (ROMIC-BDChange) and under grant no. 01LG1222A (ROMIC-TRIP). For parts of the work, FP was funded by the Helmholtz Young Investigators group A-SPECi (Assessment of stratospheric processes and their effects on climate variability). We thank ECMWF for providing reanalysis data. We acknowledge support by the Deutsche Forschungsgemeinschaft and the Open Access Publishing Fund of the Karlsruhe Institute of Technology.

The article processing charges for this open-access publication were covered by a Research Centre of the Helmholtz Association.



References

- Austin, J. and Li, F.: On the relationship between the strength of the Brewer-Dobson circulation and the age of stratospheric air, *Geophys. Res. Lett.*, 33, L17807, doi:10.1029/2006GL026867, 2006.
- Austin, J., Wilson, J., Li, F., and Vömel, H.: Evolution of water vapor and age of air in coupled chemistry climate model simulations of the stratosphere, *J. Atmos. Sci.*, 64, 905–921, 2007.
- Birner, T. and Bönisch, H.: Residual circulation trajectories and transit times into the extratropical lowermost stratosphere, *Atmos. Chem. Phys.*, 11, 817–827, doi:10.5194/acp-11-817-2011, 2011.
- Bönisch, H., Engel, A., Birner, T., Hoor, P., Tarasick, D. W., and Ray, E. A.: On the structural changes in the Brewer-Dobson circulation after 2000, *Atmos. Chem. Phys.*, 11, 3937–3948, doi:10.5194/acp-11-3937-2011, 2011.
- Calvo, N., Garcia, R. R., Randel, W. J., and Marsh, D. R.: Dynamical mechanism for the increase in tropical upwelling in the lowermost tropical stratosphere during warm ENSO events, *J. Atmos. Sci.*, 67, 2331–2340, 2010.
- Chirkov, M., Stiller, G. P., Laeng, A., Kellmann, S., von Clarmann, T., Boone, C., Elkins, J. W., Engel, A., Glatthor, N., Grabowski, U., Harth, C. M., Kiefer, M., Kolonjari, F., Krummel, P. B., Linden, A., Lunder, C. R., Miller, B. R., Montzka, S. A., Mühle, J., O'Doherty, S., Orphal, J., Prinn, R. G., Toon, G., Vollmer, M. K., Walker, K. A., Weiss, R. F., Wiecele, A., and Young, D.: Global HCFC-22 measurements with MIPAS: retrieval, validation, global distribution and its evolution over 2005–2012, *Atmos. Chem. Phys.*, 16, 3345–3368, doi:10.5194/acp-16-3345-2016, 2016.
- Eckert, E., von Clarmann, T., Kiefer, M., Stiller, G. P., Lossow, S., Glatthor, N., Degenstein, D. A., Froidevaux, L., Godin-Beekmann, S., Leblanc, T., McDermid, S., Pastel, M., Steinbrecht, W., Swart, D. P. J., Walker, K. A., and Bernath, P. F.: Drift-corrected trends and periodic variations in MIPAS IMK/IAA ozone measurements, *Atmos. Chem. Phys.*, 14, 2571–2589, doi:10.5194/acp-14-2571-2014, 2014.
- Engel, A., Möbius, T., Bönisch, H., Schmidt, U., Heinz, R., Levin, I., Atlas, E., Aoki, S., Nakazawa, T., Sugawara, S., Moore, F., Hurst, D., Elkins, J., Schauffler, S., Andrews, A., and Boering, K.: Age of stratospheric air unchanged within uncertainties over the past 30 years, *Nature Geosci.*, 2, 28–31, doi:10.1038/ngeo388, 2009.
- Fischer, H., Birk, M., Blom, C., Carli, B., Carlotti, M., von Clarmann, T., Delbouille, L., Dudhia, A., Ehhalt, D., Endemann, M., Flaud, J. M., Gessner, R., Kleinert, A., Koopmann, R., Langen, J., López-Puertas, M., Mosner, P., Nett, H., Oelhaf, H., Perron, G., Remedios, J., Ridolfi, M., Stiller, G., and Zander, R.: MIPAS: an instrument for atmospheric and climate research, *Atmos. Chem. Phys.*, 8, 2151–2188, 2008.
- Garcia, R. R. and Randel, W. J.: Acceleration of the Brewer-Dobson Circulation due to Increases in Greenhouse Gases, *J. Atmos. Sci.*, 65, 2731–2739, doi:10.1175/2008JAS2712.1, 2008.
- Garfinkel, C. I., Aquila, V., Waugh, D. W., and Oman, L. D.: Time varying changes in the simulated structure of the Brewer Dobson Circulation, *Atmos. Chem. Phys. Discuss.*, doi:10.5194/acp-2016-523, in review, 2016.
- Garny, H., Birner, T., Bönisch, H., and Bunze, F.: The effects of mixing on age of air, *J. Geophys. Res. Atmos.*, 119, 7015–7034, doi:10.1002/2013JD021417, 2014.
- Gebhardt, C., Rozanov, A., Hommel, R., Weber, M., Bovensmann, H., Burrows, J. P., Degenstein, D., Froidevaux, L., and Thompson, A. M.: Stratospheric ozone trends and variability as seen by sciamachy from 2002 to 2012, *Atmos. Chem. Phys.*, 14, 831–846, 2014.
- Glatthor, N., Höpfner, M., Leyser, A., Stiller, G. P., von Clarmann, T., Grabowski, U., Kellmann, S., Linden, A., Sinnhuber, B.-M., Krysztofiak, G., and Walker, K. A.: Global carbonyl sulfide (OCS) measured by MIPAS/Envisat during 2002–2012, *Atmos. Chem. Phys. Discuss.*, doi:10.5194/acp-2016-710, in review, 2016.



- Gray, L. J. and III, J. M. R.: Interannual variability of trace gases in the subtropical winter stratosphere, *J. Atmos. Sci.*, 56, 977–993, 1999.
- Haenel, F. J., Stiller, G. P., von Clarmann, T., Funke, B., Eckert, E., Glatthor, N., Grabowski, U., Kellmann, S., Kiefer, M., Linden, A., and Reddmann, T.: Reassessment of MIPAS age of air trends and variability, *Atmos. Chem. Phys.*, 15, 13 161–13 176, doi:10.5194/acp-15-13161-2015, 2015.
- 5 Hardiman, S. C., Butchart, N., and Calvo, N.: The morphology of the Brewer–Dobson circulation and its response to climate change in CMIP5 simulations, *Q. J. R. Meteorol. Soc.*, 140, 1958–1965, 2013.
- Harrison, J. J., Chipperfield, M. P., Boone, C. D., Dhomse, S. S., Bernath, P. F., Froidevaux, L., Anderson, J., and III, J. R.: Satellite observations of stratospheric hydrogen fluoride and comparisons with SLIMCAT calculations, *Atmos. Chem. Phys.*, 16, 10 501–10 519, doi:10.5194/acp-16-10501-2016, 2016.
- 10 Kellmann, S., von Clarmann, T., Stiller, G. P., Eckert, E., Glatthor, N., Höpfner, M., Kiefer, M., Orphal, J., Funke, B., Grabowski, U., Linden, A., Dutton, G. S., and Elkins, J. W.: Global CFC-11 (CCl_3F) and CFC-12 (CCl_2F_2) Measurements with the Michelson Interferometer for Passive Atmospheric Sounding (MIPAS): retrieval, climatologies and trends, *Atmos. Chem. Phys.*, 12, 11 857–11 875, doi:10.5194/acp-12-11857-2012, 2012.
- Lambert, A., Read, W. G., Livesey, N. J., Santee, M. L., Manney, G. L., Froidevaux, L., Wu, D. L., Schwartz, M. J., Pumphrey, H. C., Jimenez, C., Nedoluha, G. E., Cofield, R. E., Cuddy, D. T., Daffer, W. H., Drouin, B. J., Fuller, R. A., Jarnot, R. F., Knosp, B. W., Pickett, H. M., Perun, V. S., Snyder, W. V., Stek, P. C., Thurstans, R. P., Wagner, P. A., Waters, J. W., Jucks, K. W., Toon, G. C., Stachnik, R. A., Bernath, P. F., Boone, C. D., Walker, K. A., Urban, J., Murtagh, D., Elkins, J. W., and Atlas, E.: Validation of the Aura Microwave Limb Sounder middle atmosphere water vapor and nitrous oxide measurements, *J. Geophys. Res.*, 112, D24S36, doi:10.1029/2007JD008724, 2007.
- 15 Mahieu, E., Chipperfield, M. P., Notholt, J., Reddmann, T., Anderson, J., Bernath, P. F., Blumenstock, T., Coffey, M. T., Dhomse, S. S., Feng, W., Franco, B., Froidevaux, L., Griffith, D. W. T., Hannigan, J. W., Hase, F., Hossaini, R., Jones, N. B., Morino, I., Murata, I., Nakajima, H., Palm, M., Paton-Walsh, C., Russell III, J. M., Schneider, M., Servais, C., Smale, D., and Walker, K. A.: Recent northern hemisphere stratospheric HCl increase due to atmospheric circulation changes, *Nature*, 515, 104–107, 2014.
- McKenna, D. S., Konopka, P., Groöf, J.-U., Günther, G., Müller, R., Spang, R., Offermann, D., and Orsolini, Y.: A new Chemical Lagrangian Model of the Stratosphere (CLaMS) 1. Formulation of advection and mixing, *J. Geophys. Res.*, 107, doi:10.1029/2000JD000114, 2002.
- 25 McLandress, C. and Shepherd, T. G.: Simulated anthropogenic changes in the Brewer–Dobson circulation, including its extension to high latitudes, *J. Clim.*, 22, 1516–1540, doi:10.1175/2008JCLI2679.1, 2009.
- Miyazaki, K. and Iwasaki, T.: The gradient genesis of stratospheric trace species in the subtropics and around the polar vortex, *J. Atmos. Sci.*, 65, 490–508, 2007.
- 30 Nedoluha, G. E., Boyd, I. S., Parrish, A., Gomez, R. M., Allen, D. R., Froidevaux, L., Connor, B. J., and Querel, R. R.: Unusual stratospheric ozone anomalies observed in 22 years of measurements from lauder, new zealand, *Atmos. Chem. Phys.*, 15, 6817–6826, 2015a.
- Nedoluha, G. E., Siskind, D. E., Lambert, A., and Boone, C.: The decrease in mid-stratospheric tropical ozone since 1991, *Atmos. Chem. Phys.*, 15, 4215–4224, 2015b.
- Oberländer-Hayn, S., Gerber, E. P., Abalichin, J., Akiyoshi, H., Kerschbaumer, A., Kubin, A., Kunze, M., Langematz, U., Meul, M., Michou, M., Morgenstern, O., and Oman, L. D.: Is the Brewer–Dobson circulation increasing or moving upward?, *Geophys. Res. Lett.*, 43, 1772–1779, doi:10.1002/2015GL067545, 2016.
- Oman, L., Waugh, D. W., Pawson, S., Stolarski, R. S., and Newman, P. A.: On the influence of anthropogenic forcings on changes in the stratospheric mean age, *J. Geophys. Res.*, 114, D03105, doi:10.1029/2008JD010378, 2009.



- Palazzi, E., Fierli, F., Stiller, G. P., and Urban, J.: Probability density functions of long-lived tracer observations from satellite in the subtropical barrier region: data intercomparison, *Atmos. Chem. Phys.*, 11, 10 579–10 598, doi:10.5194/acp-11-10579-2011, 2011.
- Pawson, S., Steinbrecht, W., Charlton-Perez, A., Fujiwara, M., Karpechko, A., Petropavlovskikh, I., Urban, J., and Weber, M.: Update on global ozone: Past, present, and future, in: Chapter 2 in Scientific Assessment of Ozone Depletion: 2014, Global Ozone Research and Monitoring Project— Report No. 55, World Meteorological Organization, Geneva, Switzerland, 2014.
- 5 Pliener, J., von Clarmann, T., Stiller, G. P., Grabowski, U., Glatthor, N., Kellmann, S., Linden, A., Haenel, F., Kiefer, M., Höpfner, M., Laeng, A., and Lossow, S.: Methane and nitrous oxide retrievals from MIPAS-ENVISAT, *Atmos. Meas. Tech.*, 8, 4657–4670, doi:10.5194/amt-8-4657-2015, 2015.
- Pliener, J., Laeng, A., Lossow, S., von Clarmann, T., Stiller, G. P., Kellmann, S., Linden, A., Kiefer, M., Walker, K. A., Noël, S., Hervig, M., McHugh, M., Lambert, A., Urban, J., Elkins, J. W., and Murtagh, D.: Validation of revised methane and nitrous oxide profiles from MIPAS-ENVISAT, *Atmos. Meas. Tech.*, 9, 765–779, doi:10.5194/amt-9-765-2016, 2016.
- 10 Ploeger, F., Abalos, M., Birner, T., Konopka, P., Legras, B., Müller, R., and Riese, M.: Quantifying the effects of mixing and residual circulation on trends of stratospheric mean age of air, *Geophys. Res. Lett.*, 42, 2047–2054, doi:10.1002/2014GL062927, 2015a.
- Ploeger, F., Riese, M., Haenel, F., Konopka, P., Müller, R., and Stiller, G.: Variability of stratospheric mean age of air and of the local effects of residual circulation and eddy mixing, *J. Geophys. Res. Atmos.*, 120, 716–733, doi:10.1002/2014JD022468, 2015b.
- 15 Pommrich, R., Müller, R., Groß, J.-U., Konopka, P., Ploeger, F., Vogel, B., Tao, M., Hoppe, C. M., Günther, G., Spelten, N., Hoffmann, L., Pumphrey, H.-C., Viciani, S., D’Amato, F., Volk, C. M., Hoor, P., Schlager, H., and Riese, M.: Tropical troposphere to stratosphere transport of carbon monoxide and long-lived trace species in the Chemical Lagrangian Model of the Stratosphere (CLaMS), *Geosci. Model Dev.*, 7, 2895–2916, 2014.
- 20 Ray, E. A., Moore, F. L., Rosenlof, K. H., Davis, S. M., Boenisch, H., Morgenstern, O., Smale, D., Rozanov, E., Hegglin, M., Pitari, G., Mancini, E., Braesicke, P., Butchart, N., Hardiman, S., Li, F., Shibata, K., and Plummer, D. A.: Evidence for changes in stratospheric transport and mixing over the past three decades based on multiple data sets and tropical leaky pipe analysis, *J. Geophys. Res.*, 115, D21304, doi:10.1029/2010JD014206, 2010.
- Shuckburgh, E., Norton, W., Iwi, I., and Haynes, P.: The influence of the quasi-biennial oscillation on isentropic transport and mixing in the tropics and subtropics, *J. Geophys. Res.*, 106, 14 327–14 338, 2001.
- 25 SPARC CCMVal: Neu, J. and S. Strahan, Chapter 5. Transport, in: SPARC Report on the Evaluation of Chemistry-Climate Models, edited by Eyring, V., Shepherd, T. G., and Waugh, D. W., SPARC Report No. 5, WCRP-132, WMO/TD-No. 1526, <http://www.atmosp.physics.utoronto.ca/SPARC>, 2010.
- Sparling, L. C.: Statistical perspectives on stratospheric transport, *Rev. Geophys.*, 38, 417–436, doi:10.1029/1999RG000070, 2000.
- 30 Stiller, G. P., von Clarmann, T., Haenel, F., Funke, B., Glatthor, N., Grabowski, U., Kellmann, S., Kiefer, M., Linden, A., Lossow, S., and López-Puertas, M.: Observed temporal evolution of global mean age of stratospheric air for the 2002 to 2010 period, *Atmos. Chem. Phys.*, 12, 3311–3331, doi:10.5194/acp-12-3311-2012, 2012.
- Waugh, D.: The age of stratospheric air, *Nature Geoscience*, 2, 14–16, 2009.
- Waugh, D. W. and Hall, T. M.: Age of stratospheric air: theory, observations, and models, *Rev. Geophys.*, 40, 1010, doi:10.1029/2000RG000101, 2002.
- 35